



Published in final edited form as:

J Med Chem. 2011 March 24; 54(6): 1555–1564. doi:10.1021/jm101323b.

Synthesis and Pharmacological Evaluation of Fluorine Containing D₃ Dopamine Receptor Ligands

Zhude Tu[†], Shihong Li[†], Jinquan Cui[†], Jinbin Xu[†], Michelle Taylor^{||}, David Ho^{||}, Robert R. Luedtke^{||}, and Robert H. Mach^{*,†,‡,§}

[†] Department of Radiology, Washington University School of Medicine, St. Louis, MO 63110

[‡] Cell Biology & Physiology, Washington University School of Medicine, St. Louis, MO 63110

[§] Biochemistry & Molecular Biophysics, Washington University School of Medicine, St. Louis, MO 63110

^{||} Department of Pharmacology and Neuroscience, University of North Texas Health Science Center, Fort Worth, TX 76107, USA

Abstract

A series of fluorine containing *N*-(2-methoxyphenyl)piperazine and *N*-(2-fluoroethoxy)piperazine analogues were synthesized and their affinities for human dopamine D₂, D₃ and D₄ receptors were determined. Radioligand binding studies identified five compounds, **18a**, **20a**, **20c**, **20e** and **21e**, which bind with high affinity at D₃ ($K_i = 0.17$ to 5 nM) and moderate to high selectivity for D₃ vs. D₂ receptors (ranging from ~25 to 163-fold). These compounds were also evaluated for intrinsic activity at D₂ and D₃ receptors using a forskolin-dependent adenylyl cyclase assay. This panel of compounds exhibits varying receptor subtype binding selectivity and intrinsic activity at D₂ vs. D₃ receptors. These compounds may be useful for behavioral pharmacology studies on the role of D₂-like dopamine receptors in neuropsychiatric and neurological disorders. Furthermore, compound **20e**, which has the highest binding affinity and selectivity for the D₃ receptor ($K_i = 0.17$ nM for D₃, 163-fold selectivity for D₃ vs. D₂ receptors) represents a candidate fluorine-18 radiotracer for *in vivo* PET imaging studies on the regulation of D₃ receptor expression.

Introduction

Dopamine receptors are G protein-coupled receptors and are classified into two major types, the D₁-like and D₂-like receptors. The D₁-like receptor subtypes include the D₁ (rat D_{1a}) and D₅ (rat D_{1b}) receptors, whereas the D₂-like receptor subtypes include the D₂, D₃ and D₄ receptors. Agonist stimulation of D₁-like receptors results in an activation of adenylyl cyclase. Stimulation of D₂-like receptors results in an inhibition of adenylyl cyclase activity, an increase in the release of arachidonic acid, activation of G protein-coupled inwardly-rectifying potassium channels (GIRKs), activation of phospholipase D (PLD) and also an increase in phosphatidylinositol hydrolysis.¹ D₂ and D₃ receptors have ~46% overall amino acid sequence homology and 78% sequence homology within the transmembrane spanning segments.²

* To whom correspondence should be addressed: Robert H. Mach, Ph.D., Division of Radiological Sciences, Washington University School of Medicine, Campus Box#: 8225, 510 South Kingshighway, St. Louis, MO 63110, Phone: (314) 362-8538, Fax: (314) 362-0039, rhmach@mir.wustl.edu.

Supporting Information Available. Experimental procedures and analytical data for compounds **9a–e**, **10a–c**, **11a**, **11b**, **12a**, **12b**, **14**, **16a–f** and **17a–d**, HPLC conditions to confirm the purity of final compounds, and elemental analysis data on all new compounds are available free of charge via the Internet at <http://pubs.acs.org>.

There is a large body of evidence indicating that D₃ dopamine receptors may play an important role in a number of neurological and neuropsychiatric disorders.³ First, the high density of D₃ receptors in limbic regions⁴⁻⁷ suggests that this receptor subtype may play a role in the etiology of schizophrenia and that D₃-selective antagonists may exhibit an antipsychotic profile devoid of extrapyramidal side effects.^{2, 5, 7} Second, prolonged treatment of 6-hydroxydopamine unilaterally lesioned rats with L-DOPA is a rodent model of L-DOPA-induced dyskinesia (LID); previous studies have suggested that there is an upregulation of D₃ receptors in dyskinetic animals.⁸⁻¹⁰ D₃ receptor selective ligands have been shown to be effective in attenuating L-DOPA-induced dyskinesia in rats, suggesting that the D₃ receptor may be an important therapeutic target for the treatment of LID.¹¹⁻¹⁵ Finally, the positive reinforcing effects of psychostimulants, such as cocaine and methamphetamine, may be mediated, in part, by the stimulation of D₃ receptors. Therefore, D₃ receptor selective partial agonists and/or antagonists may be useful pharmacotherapeutic agents for the treatment of substance abuse.¹⁶⁻²¹

Positron Emission Tomography (PET) is a non-invasive imaging technique that has been used to study the expression of dopamine receptors in the brain. However, the identification of D₃ receptor specific PET radioligands has been challenging because of the high degree of amino acid sequence homology between D₂ and D₃ receptor binding sites in the ligand binding domain.^{1, 20,3, 22-25} A number of D₃-selective ligands have served as lead compounds for PET radiotracer development (Figure 1).²⁶⁻³⁰ Unfortunately, none of the D₃ receptor selective radiotracers reported to date have shown promise in *in vivo* imaging or brain uptake studies in rodents or nonhuman primates. One of the main limitations of many D₃-selective ligands is their relatively high lipophilicity, which could compromise their ability to cross the blood-brain barrier and label D₃ receptors *in vivo*.

Over the past decade, our group has focused on identifying candidate ligands having the right balance between D₃ receptor affinity (1-5 nM), selectivity (>50-fold selective for D₃ versus D₂ receptors), and lipophilicity (log P = 2.0 – 4.0) to give a suitable signal: noise ratio in PET imaging studies. We previously reported benzamide analogues, **1** (WC-10) (K_i = 0.8 nM for D₃ receptor, D₂/D₃ ratio = 43) and **2** (WC-44) (K_i = 2.4 nM for D₃, D₂/D₃ ratio = 23) as lead compounds for radiotracer development.²⁴ Quantitative autoradiography studies using [³H]-**1** demonstrated it has high affinity and moderate selectivity for D₃ vs. D₂ receptor,^{24, 31} which is consistent with *in vitro* screening data using competition binding assays.²⁵ However, microPET studies of [¹¹C]-**1** in rhesus brain have exhibited high levels of variability for D₃ imaging between subjects, and similar studies using [¹⁸F]-**2** have not shown good target to non-target ratios.²⁵

Our laboratory has continued to investigate the structure-activity relationships of conformationally flexible benzamide analogues by optimizing the structures of **1** and **2** to identify promising candidates for imaging the D₃ receptor with PET. The longer half-life of ¹⁸F ($t_{1/2}$ = 109.8 min) compared to ¹¹C ($t_{1/2}$ = 20.4 min) places fewer time constraints on radiotracer synthesis and permits longer scan sessions for ¹⁸F-labeled radiotracers versus ¹¹C-labeled radiotracers. In this article, we report the synthesis and *in vitro* evaluation of a series of fluorine containing conformationally flexible benzamide analogues, in which the structure was altered by: 1) replacing the 2-methoxyphenyl group in the piperazinyl ring with a 2-(2-fluoroethoxyphenyl) group; 2) introducing a 2-fluoroethoxy or 2-fluoroethyl group in the 2- and 4-position of the benzamide moiety; and, 3) comparing the effect of having a double bond (*trans*-butenyl) within the four carbon chain that links the arylamide with the 4-phenylpiperazine moiety.

Results and Discussion

Chemistry

The target compounds were synthesized as depicted in Schemes 1–3. The synthesis of the substituted benzoic acids (**9a–e**) was accomplished as outlined in Scheme 1. The acids were first converted into the corresponding methyl esters by Fischer esterification. *O*-alkylation of 2-hydroxyl or 4-hydroxyl group was achieved by treatment with 1-bromo-2-fluoroethane in acetone using potassium carbonate as the base. Hydrolysis of the methyl ester with sodium hydroxide in aqueous methanol afforded the corresponding 2-fluoroethoxy benzoic acids **9a–e**. The synthesis of the 4-fluoropegylated benzoic acids **12a** and **12b** is shown in Scheme 2. *O*-alkylation of the phenol group of 4-hydroxy-benzoic acid methyl ester with either 2-(2-chloroethoxy)ethanol or 2-(2-(2-chloroethoxy)ethoxy)ethanol in the presence of potassium carbonate in tetrahydrofuran afforded **10a** and **12b** (Scheme 2). Conversion of alcohols **10a** and **10b** to the corresponding fluoro derivatives **11a** and **11b** was accomplished using two different methods. Direct conversion of the hydroxyl group of **10a** with diethylaminosulfur trifluoride (DAST) gave **11a** in modest yield (43%). Alternatively, conversion of the hydroxyl group of **10b** to the corresponding tosylate group, **10c**, followed by displacement with tetrabutylammonium fluoride (TBAF) gave **11b** in an overall yield of 56%. Hydrolysis of **11a** and **11b** with sodium hydroxide in aqueous methanol afforded benzoic acids **12a** and **12b**.

The substituted 4-(4-phenylpiperazin-1-yl)butan-1-amines (**17a, b**) and the substituted 4-(4-phenylpiperazin-1-yl)-*trans*-but-2-en-1-amines (**17b, d**) were synthesized according to Scheme 3. Treatment of potassium 1,3-dihydro-1,3-dioxoisindole (**13**) with *trans*-1,4-dibromo-2-butene in *N,N*-dimethylformamide (DMF) gave 2-(*trans*-4-bromobut-2-enyl)-1,3-dihydro-1,3-dioxoisindole, **14**, in modest yield (69%). The *N*-alkylation of 1-(2-methoxyphenyl)piperazine (**15a**) or 1-(2-hydroxyphenyl)piperazine (**15b**) with either 2-(4-bromobutyl)-1,3-dihydro-1,3-dioxoisindole or **14** produced **16a–d**. *O*-alkylation of the phenol group in **16b** and **16d** with 1-bromo-2-fluoroethane in acetone using potassium carbonate as the base afforded compounds **16e,f**. Treatment of **16a, c** and **16e,f** with hydrazine in refluxing ethanol (Scheme 3) afforded the corresponding amines **17a–d** in variable yields.

The target benzamides **18a–c**, **19a–g**, **20b–d,f** and **21b–d**, were synthesized by coupling amines **17a–d** with substituted benzoic acids **9a–e**, **12a–b** and 4-(2-fluoroethyl)benzoic acid, ²⁵ with *N,N'*-dicyclohexyl-carbodiimide (DCC) in dichloromethane (Scheme 4). Benzamides **20a e** and **21a,e**, were prepared by coupling amines **17b,d** with the corresponding commercially available benzoic acid. All final compounds were converted into the corresponding oxalic acid salt for *in vitro* binding studies.

In Vitro Binding Studies

Compounds were first evaluated for affinity at human D₂ and D₃ dopamine receptors expressed in stably transfected HEK cells. Analogues which exhibited high binding affinity at D₃ receptors were further evaluated for affinity at a) D₄ dopamine receptors and b) σ₁ and σ₂ sigma receptors. The σ receptor binding studies were undertaken because of the ubiquitous expression of sigma receptors in the CNS. Therefore, high σ₁ or σ₂ receptor binding affinity would preclude the usefulness of a D₃-selective radiotracer for PET imaging studies. The σ receptor binding studies were included to ensure that our compounds bind with low affinity for σ receptors.

The [¹²⁵I]-IABN inhibition constants (K_i) at D₂ and D₃ receptors are reported in Table 1. The ligand binding selectivity, in terms of a selectivity index, is calculated as $K_i(D_2)/K_i$

(D₃). For the ensuing discussion, binding affinities are characterized as very high ($K_i < 1.0$ nM), high ($K_i = 1-10$ nM), moderate ($K_i = 11-50$ nM) or low ($K_i > 50$ nM).

The radioligand binding assays identified a number of potentially useful structure-activity trends as well as several promising fluorinated analogues which could serve as potential PET radiotracers. First, in a comparison of **1** and **18a-c**, it was observed that replacing the 4-dimethylamino group in the benzamide moiety with a 4-(2-fluoroethoxy) group (compound **18a**) resulted in a D₃ binding affinity ($K_i = 1.1$ nM) comparable to **1** ($K_i = 0.8$ nM). However, there was a decrease in D₃ receptor affinity when the 4-(2-fluoroethoxy) group was homologated to the corresponding fluoropegylated groups, **18b** and **18c**. Thus, the D₃ vs. D₂ selectivity for **18b** and **18c**, was <15-fold, whereas the D₃ vs. D₂ selectivity for **18a** was ~25 fold.

To further explore the structure-activity relationships of this series, the structures of the amides were modified by introducing the 2-fluoroethoxyl group in the 2-position compared to 4-position of the benzamide moiety. These analogs also had a methyl or halogen atom (Br or I) in the 5-position, and the *trans* double bond 4-carbon spacer group. This approach generally resulted in compounds with only moderate affinity for both D₃ and D₂ receptors (compounds **19d-f**), except for compound **19g** which displayed a 4-fold selectivity for D₃ versus D₂ receptors. Based on these results, a higher D₃ receptor affinity and selectivity was observed when the 2-fluoroethoxy is in the 4-position of the benzamide region (compound **19b**) rather than the 2-position.

The next substitution involved replacing the 2-methoxy group with a 2-fluoroethoxy group in the *N*-phenylpiperazinyl moiety. The replacement of a methoxy group with a 2-fluoroethoxy group is a standard method for preparing a potential ¹⁸F-labeled radiotracer. This modification generally resulted in compounds having a slightly increased D₃ binding affinity when compared with the corresponding *N*-(2-methoxyphenyl)piperazinyl analogs (e.g., **20a** vs. **1**, **20c** vs. **18a** and **20d** vs. **18c**). However, one exception to this trend was noticed, with **20b** having a lower D₃ affinity than its corresponding 2-methoxy analog, **2**. An interesting observation was in the substitution of the 4-position of the benzamide group with a 3-thiophene ring to give compound **20e**; this analog displayed both the highest D₃ binding affinity (0.17 nM) and greatest D₃ vs. D₂ receptor selectivity (163-fold) among the compounds reported in this article.

When the saturated 4-carbon spacer linking the arylamide with the *N*-(4-methoxyphenyl)piperazine moiety was replaced with a *trans* double bond, the binding affinity at both D₂ and D₃ receptors generally decreased. However, replacing the single bond with a *trans* double bond caused a larger reduction in D₃ affinity relative to the reduction in D₂ affinity. This trend was also observed with the *N*-(2-fluoroethoxyphenyl)piperazine containing analogues shown in Table 1. These results are consistent with the *N*-(2-methoxyphenyl)piperazinyl analogs described by Taylor et al.³² but opposite to what has been reported with the corresponding *N*-(2,3-dichlorophenyl)piperazinyl benzamide analogs.^{20, 33} Therefore, the effect of the single vs. double bond replacement on binding selectivity appears to be governed by the type of substitution on the *N*-phenylpiperazine group. The only analog showing an increase in D₃ affinity when the *trans* double bond was introduced was **21b**, which had a 6-fold higher affinity at D₃ receptors when compared with its saturated analog **20b**.

Affinity at dopamine D₄ receptors was determined on compounds having a high affinity ($K_i < 5$ nM) for D₃ receptors and high selectivity for D₃ vs. D₂ receptors (>10 fold). All compounds that were tested exhibited low binding affinity at D₄ receptors (Table 1).

Since many dopamine ligands have been shown to bind to σ_1 and σ_2 receptors, we determined the σ receptor binding affinities for compounds having a high D₃ receptor affinity and good selectivity for D₃ vs. D₂ receptors. All of the compounds tested exhibited low binding affinities at σ_1 and σ_2 receptors. The affinity ratios of D₃ to σ receptors were >260-fold (Table 2). Compound **20e**, which has the highest D₃ affinity and D₃ vs. D₂ selectivity ratio, binds with low affinity at both σ_1 and σ_2 receptors. This observation eliminates any concern that σ receptor binding might interfere with the imaging signal when a ¹⁸F-radiolabeled derivative of **20e** is made for PET imaging studies of the D₃ receptor.

Intrinsic Activity at Dopamine Receptors

The intrinsic activity of compounds **18a**, **18c**, **20a**, **20c**, **20e**, **21b**, and **21e** at D₃ and D₂ receptors was also evaluated. This assay measures the ability of the compounds to inhibit forskolin-dependent stimulation of adenylyl cyclase activity in stably transfected HEK-293 cells expressing human D₂ or D₃ dopamine receptors. For each compound, the inhibition was compared to the intrinsic efficacy of the full agonist quinpirole and the antagonist haloperidol. The compounds that were evaluated were all partial agonists at D₃ dopamine receptors, displaying intrinsic efficacy from 34.5 ± 1.7 % (**20e**) to 68.8 ± 5.6% (**18a**) (Table 3). As previously reported, the constituent at the *para* position of the benzamide group plays a pivotal role in determining the intrinsic activity of our compounds. For example, **1**, **2**, **18a** and **18c** each contain a 4-(2-methoxyphenyl)piperazine moiety with a saturated 4-carbon spacer, yet their efficacy compared to quinpirole varies from 34% to 64% at D₂ receptors and 18% to 96% at D₃ receptors. In addition, the structure of the 4-carbon spacer influences efficacy. For example, substitution of a *trans* double bond (**21e**) for the saturated spacer (**20e**) had minimal effect on efficacy at D₂ receptors (29% vs. 21% maximal efficacy), while efficacy at D₃ receptors increased almost 60% (35% to 55% maximal efficacy) (Table 3). The diverse range of D₃ and D₂ receptor affinities and intrinsic activities at these receptors indicates that these compounds are useful probes for studying the behavioral pharmacology of D₃ and D₂ receptors in animal models of substance abuse, schizophrenia, and L-DOPA induced dyskinesia. In addition, since most dopamine receptor imaging agents have been either antagonists (e.g., [¹¹C]raclopride and [¹⁸F]fallypride) or full agonists (e.g., [¹¹C]-(+)-4-propyl-9-hydroxynaphthoxazine ([¹¹C](+)-PHNO) and [¹¹C]-*N*-propylapomorphine ([¹¹C]NPA)) at both D₂ and D₃ receptors, it will be of interest to see if the partial agonists described here are capable of serving as radiotracers for imaging the D₃ receptor in vivo with PET.

In summary, we observed that the 2-methoxy group in the 4-(2-methoxyphenyl)piperazinyl moiety can be replaced with a 2-fluoroethoxy group, a commonly-used strategy for preparing ¹⁸F-labeled PET radiotracers, without causing a significant change in D₃ receptor affinity or D₃ vs. D₂ selectivity ratio. An exception to this trend were the structural congeners which contained the 4-(2-fluoroethyl)benzamide moiety: **21b** had a much *higher* D₃ affinity than its 4-(2-methoxyphenyl)piperazine analogue, **19a** (K_i = 1.1 ± 0.2 nM vs. 24.9 ± 3.3 nM, respectively), and **20b**, which had a *lower* D₃ affinity and poorer D₃ vs. D₂ selectivity ratio than its corresponding 4-(2-methoxyphenyl)piperazine analogue, **2**. Replacing the saturated 4-carbon spacer that links the benzamide and the 4-phenylpiperazinyl moieties with a *trans* double bond reduced the binding affinity at D₃ and D₂ receptors. However, the presence of the *trans* double bond can modulate the intrinsic efficacy of the analogue. Finally, although increasing the length of the 2-fluoroethoxy side chain by pegylation did not dramatically alter the D₃ binding affinity or the D₃ vs. D₂ receptor binding selectivity, it did decrease the log P value, which may facilitate the penetration of blood-brain-barrier.

Conclusion

In the present study, we have reported the synthesis and pharmacological evaluation of a series of benzamides which have high binding affinity for D₃ receptors and good selectivity for D₃ vs. D₂ receptors. Within the series, 5 compounds exhibited high D₃ binding affinity (≤ 5.0 nM) and/or moderate to high selectivity for D₃ vs. D₂ receptors, including **18a**, **20a**, **20c**, **20e** and **21e**. Moreover, all of these analogues contain a fluorine atom, thus providing candidates ligands for PET imaging studies via the corresponding ¹⁸F-labeled analogs.

Since recent studies indicate that the density of D₃ receptors in the striatal regions of brain is ~40% that of the D₂ receptor³², ligands having a high D₃ versus D₂ selectivity (>50-fold) will likely be needed in order to image D₃ versus D₂ receptors in the CNS. Among the 5 compounds described above, **20e** displayed the highest D₃ affinity (0.17 nM) and selectivity for D₃ vs. D₂ receptors (163-fold). However, the high lipophilicity of this analog (log P = 4.67) may limit its utility as a PET radiotracer because of its predicted low brain uptake and relatively high level of nonspecific binding. *In vivo* evaluation of a number of the fluorinated ligands described above are currently ongoing to assess their suitability for use as PET tracers for studying the *in vivo* expression and regulation of D₃ dopamine receptors in the CNS.

Experimental Section

General

4-Dimethylaminobenzoic acid was purchased from Sigma-Aldrich (Milwaukee, WI) and 3-thienylbenzoic acid Matrix Scientific (Columbia, SC). All other synthetic intermediates were purchased from Sigma-Aldrich and used as received unless otherwise stated. Tetrahydrofuran (THF) was distilled from sodium hydride immediately prior to use.

All air-sensitive reactions were carried out in oven-dried glassware under an inert nitrogen atmosphere unless otherwise stated. Standard handling techniques for air sensitive materials were employed throughout this study. Yields were not optimized. Melting points were determined on a Haake-Buchler or Mel-Temp melting point apparatus and are uncorrected. ¹H NMR spectra were recorded at 300 MHz on a Varian Mercury-VX spectrometer with CDCl₃ as the solvent and tetramethylsilane (TMS) as the internal standard. The following abbreviations were used to describe peak patterns wherever appropriate: b = broad, d = doublet, t = triplet, q = quartet, m = multiplet. Analytical thin layer chromatography (TLC) was performed on Analtech GHLF silica gel glass plates, and visualization was aided by UV. Elemental analyses (C, H, N) were determined by Atlantic Microlab, Inc. (Norcross, GA) and the results are within 0.4% of the calculated values unless otherwise noted. The purity of the target compounds was determined by elemental analysis and by HPLC methods. All the compounds reported in this article have a purity $\geq 95\%$. The synthesis of benzoic acid intermediates **9a–e**, **12a** and **12b**, and the amine intermediates **17a–d** can be found in the Supporting Data section.

General Method for Preparing the Substituted Benzamide Analogs

4-(2-Fluoroethoxy)-N-(4-(4-(2-methoxyphenyl)-piperazin-1-yl)-butyl)benzamide (**18a**)

A mixture of compound **17a** (379 mg, 1.44 mmol) and **9a** (221 mg, 1.20 mmol) in dichloromethane (20 mL) was stirred at 0 °C (ice-water bath). Dicyclohexylcarbodiimide (DCC) (356 mg, 1.73 mmol) and hydroxybenzotriazole (HOBT) (234 mg, 1.73 mmol) were added to the above solution. Then the ice bath was removed and the reaction mixture was stirred at ambient temperature for 15 h. Dichloromethane (60 mL) was added into the reaction mixture and the solution was washed with saturated aqueous NaHCO₃ solution (3 ×

10 mL). The organic layer was dried over Na₂SO₄, concentrated under reduced pressure and the crude product was purified by silica gel column chromatography using dichloromethane/methanol (20/1, v/v) as the mobile phase to give **18a** (443 mg, 86%). Mp (oxalate salt): 151.5–152.6 °C. ¹H NMR (300 MHz, free base, CDCl₃): δ 1.61–1.69 (m, 4H), 2.48 (t, *J* = 5.2 Hz, 2H), 2.66 (s, 4H), 3.08 (s, 4H), 3.48 (q, *J* = 5.7 Hz, 2H), 3.85 (s, 3H), 4.19 (t, *J* = 4.2 Hz, 1H), 4.28 (t, *J* = 4.2 Hz, 1H), 4.68 (t, *J* = 4.2 Hz, 1H), 4.84 (t, *J* = 4.2 Hz, 1H), 6.61 (br s, 1H), 6.82–7.04 (m, 6H), 7.74 (d, *J* = 8.7 Hz, 2H). Anal. (C₂₄H₃₂FN₃O₃·1.5H₂C₂O₄) C, H, N.

4-(2-(2-Fluoroethoxy)ethoxy)-*N*-(4-(4-(2-methoxyphenyl)piperazin-1-yl)butyl)benzamide (18b)

18b was made from **12a** and **17a**. Yield: 84%. Mp (oxalate salt): 127.9–129.0 °C. ¹H NMR (free base, CDCl₃): δ 1.66–1.68 (m, 4H), 2.47 (t, *J* = 3.6 Hz, 2H), 2.65 (s, 4H), 3.08 (s, 4H), 3.47 (q, *J* = 5.4 Hz, 2H), 3.76 (t, *J* = 4.8 Hz, 1H), 3.85 (s, 3H), 3.91 (t, *J* = 3.6 Hz, 2H), 4.17 (t, *J* = 4.8 Hz, 2H), 4.52 (t, *J* = 4.2 Hz, 1H), 4.67 (t, *J* = 4.2 Hz, 1H), 6.58 (t, *J* = 10.0 Hz, 1H), 6.83–7.04 (m, 6H), 7.72 (d, *J* = 9.0 Hz, 2H). Anal. (C₂₆H₃₆FN₃O₄·H₂C₂O₄) C, H, N.

4-(2-(2-(2-Fluoroethoxy)ethoxy)ethoxy)-*N*-(4-(4-(2-methoxyphenyl)piperazin-1-yl)butyl)benzamide (18c)

18c was prepared from **12b** and **17a**. Yield: 98%. Mp (oxalate salt): 103.0–103.9 °C. ¹H NMR (free base, CDCl₃): δ 1.60 (s, 4H), 1.67 (t, *J* = 3.3 Hz, 4H), 2.47 (t, *J* = 4.8 Hz, 2H), 2.66 (s, 4H), 3.08 (s, 4H), 3.47 (q, *J* = 5.7 Hz, 2H), 3.69–3.76 (m, 4H), 3.80 (t, *J* = 4.2 Hz, 1H), 3.86 (s, 3H), 3.88 (t, *J* = 4.8 Hz, 2H), 4.16 (t, *J* = 4.8 Hz, 2H), 4.48 (t, *J* = 4.2 Hz, 1H), 4.64 (t, *J* = 4.2 Hz, 1H), 6.54 (t, *J* = 9.0 Hz, 1H), 6.83–7.04 (m, 6H), 7.72 (d, *J* = 9.0 Hz, 2H). Anal. (C₂₈H₄₀FN₃O₅·H₂C₂O₄·0.4H₂O) C, H, N.

4-(2-Fluoroethyl)-*N*-(4-(4-(2-methoxyphenyl)piperazin-1-yl)-*trans*-butyl-2-enyl)benzamide (19a)

19a was prepared from 4-(2-fluoroethyl)benzoic acid and **17c**. Yield: (397 mg, 98%). Mp (oxalate salt): 116.7–121.3 °C. ¹H NMR (free base, CDCl₃): δ 2.63 (s, 4H), 3.03 (t, *J* = 4.8 Hz, 2H), 3.08–3.12 (m, 6H), 3.85 (s, 3H), 4.06–4.08 (t, *J* = 6.2 Hz, 2H), 4.57 (t, *J* = 4.8 Hz, 1H), 4.72 (t, *J* = 4.8 Hz, 1H), 5.78 (t, *J* = 5.4 Hz, 2H), 6.80 (t, *J* = 6.3 Hz, 1H), 6.82–7.04 (m, 4H), 7.31 (d, *J* = 8.4 Hz, 2H), 7.73 (d, *J* = 8.4 Hz, 2H). Anal. (C₂₄H₃₀FN₃O₂·0.5H₂C₂O₄·H₂O) C, H, N.

4-(2-Fluoroethoxy)-*N*-(4-(4-(2-methoxyphenyl)piperazin-1-yl)-*trans*-butyl-2-enyl)benzamide (19b)

19b was prepared from **9a** and **17c**. Yield: 77%. Mp (oxalate salt): 133.6–134.9 °C. ¹H NMR (free base, CDCl₃): δ 2.67 (s, 4H), 3.08–3.09 (m, 6H), 3.86 (s, 3H), 4.09 (t, *J* = 4.3 Hz, 2H), 4.22 (t, *J* = 4.2 Hz, 1H), 4.30 (t, *J* = 4.2 Hz, 1H), 4.69 (t, *J* = 4.2 Hz, 1H), 4.85 (t, *J* = 4.2 Hz, 1H), 5.78 (t, *J* = 5.3 Hz, 2H), 6.13 (t, *J* = 6.3 Hz, 1H), 6.83–7.04 (m, 6H), 7.75 (d, *J* = 9.3 Hz, 2H). Anal. (C₂₄H₃₀FN₃O₃) C, H, N.

4-(2-(2-Fluoroethoxy)ethoxy)-*N*-(4-(4-(2-methoxyphenyl)piperazin-1-yl)-*trans*-butyl-2-enyl)benzamide (19c)

19c was prepared from **12a** and **17c**. Yield: 99%. Mp (oxalate salt): 108.3–109.8 °C. ¹H NMR (free base, CDCl₃): δ 2.67 (s, 4H), 3.07–3.10 (m, 6H), 3.77 (t, *J* = 4.2 Hz, 1H), 3.85 (s, 3H), 3.86–3.94 (m, 3H), 4.06–4.10 (m, 2H), 4.19 (m, 2H), 4.52 (t, *J* = 4.1 Hz, 1H), 4.68 (t, *J* = 4.1 Hz, 1H), 5.78 (t, *J* = 3.3 Hz, 2H), 6.10 (t, *J* = 5.3 Hz, 1H), 6.82–7.04 (m, 6H), 7.73 (d, *J* = 8.7 Hz, 2H). Anal. (C₂₆H₃₄FN₃O₄·H₂C₂O₄) C, H, N.

2-(2-Fluoroethoxy)-5-methyl-N-(4-(4-(2-methoxyphenyl)piperazin-1-yl)-trans-butyl-2-enyl)benzamide (19d)

19d was prepared from **9b** and **17c**. Yield: 79%. Mp (oxalate salt): 151.1–152.3 °C. ¹H NMR (free base, CDCl₃): δ 2.33 (s, 3H), 2.67 (s, 4H), 3.07–3.09 (m, 6H), 3.85 (s, 3H), 4.06–4.14 (m, 2H), 4.26 (t, *J* = 4.1 Hz, 1H), 4.35 (t, *J* = 4.1 Hz, 1H), 4.70 (t, *J* = 4.1 Hz, 1H), 4.86 (t, *J* = 4.1 Hz, 1H), 5.79 (t, *J* = 2.4 Hz, 2H), 6.80–7.04 (m, 5H), 7.214 (dd, *J* = 2.4, 8.7 Hz, 1H), 7.98 (br s, 1H), 8.00 (dd, *J* = 2.4, 8.7 Hz, 1H). Anal. (C₂₅H₃₂FN₃O₃·H₂C₂O₄) C, H, N.

5-Bromo-2-(2-fluoroethoxy)-N-(4-(4-(2-methoxyphenyl)piperazin-1-yl)-trans-butyl-2-enyl)benzamide (19e)

19e was prepared from **9c** and **17c**. Yield: 35%. Mp (oxalate salt): 157.6–158.7 °C. ¹H NMR (free base, CDCl₃): δ 2.65 (s, 4H), 3.06–3.10 (m, 6H), 3.85 (s, 3H), 4.09 (t, *J* = 5.1 Hz, 2H), 4.27 (t, *J* = 4.1 Hz, 1H), 4.37 (t, *J* = 4.1 Hz, 1H), 4.71 (t, *J* = 4.1 Hz, 1H), 4.87 (t, *J* = 4.1 Hz, 1H), 5.76–5.80 (m, 2H), 6.80–7.04 (m, 5H), 7.52 (dd, *J* = 2.4, 8.4 Hz, 1H), 7.61 (br s, 1H), 8.32 (d, *J* = 5.4 Hz, 1H). Anal. (C₂₄H₂₉BrFN₃O₃) C, H, N.

2-(2-Fluoroethoxy)-5-iodo-N-(4-(4-(2-methoxyphenyl)piperazin-1-yl)-trans-butyl-2-enyl)benzamide (19f)

19f was prepared from **9d** and **17c**. Yield: 60%. Mp (oxalate salt): 162.2–163.6 °C. ¹H NMR (free base, CDCl₃): δ 2.65 (s, 4H), 3.07–3.10 (m, 6H), 3.86 (s, 3H), 4.09 (t, *J* = 5.1 Hz, 2H), 4.27 (t, *J* = 4.1 Hz, 1H), 4.36 (t, *J* = 4.1 Hz, 1H), 4.72 (t, *J* = 4.1 Hz, 1H), 4.88 (t, *J* = 4.1 Hz, 1H), 5.74–5.82 (m, 2H), 6.71 (d, *J* = 8.7 Hz, 1H), 6.84–7.04 (m, 4H), 7.71 (dd, *J* = 2.4, 8.4 Hz, 1H), 7.83 (br s, 1H), 8.49 (d, *J* = 2.1 Hz, 1H). Anal. (C₂₄H₂₉FIN₃O₃·H₂C₂O₄·0.5H₂O) C, H, N.

5-Bromo-2-(2-fluoroethoxy)-3-methoxy-N-(4-(4-(2-methoxyphenyl)piperazin-1-yl)-trans-butyl-2-enyl)benzamide (19g)

19g was prepared from **9e** and **17c**. Yield: 84%. Mp (oxalate salt): 193.5–195.5 °C. ¹H NMR (free base, CDCl₃): δ 2.66 (s, 4H), 3.06–3.10 (m, 6H), 3.86 (s, 3H), 3.87 (s, 3H), 4.06 (t, *J* = 4.2 Hz, 2H), 4.27 (t, *J* = 4.1 Hz, 1H), 4.36 (t, *J* = 4.1 Hz, 1H), 4.62 (t, *J* = 3.9 Hz, 1H), 4.78 (t, *J* = 3.9 Hz, 1H), 5.76 (t, *J* = 3.3 Hz, 2H), 6.84–7.04 (m, 4H), 7.14 (d, *J* = 2.4 Hz, 1H), 7.88 (d, *J* = 2.1 Hz, 1H), 8.04 (br s, 1H). Anal. (C₂₅H₃₁BrFN₃O₄·H₂C₂O₄) C, H, N.

4-(Dimethylamino)-N-(4-(4-(2-(2-fluoroethoxy)phenyl)piperazin-1-yl)butyl)benzamide (20a)

20a was prepared from 4-dimethylaminobenzoic acid and **17b**. Yield: 80%. Mp (oxalate salt): 103.4–106.3 °C. ¹H NMR (free base, CDCl₃): δ 1.60–1.80 (m, 4H), 2.45 (t, *J* = 2.1 Hz, 2H), 2.65 (s, 4H), 3.00 (s, 6H), 3.12 (s, 4H), 3.46 (q, *J* = 5.4 Hz, 2H), 4.19 (t, *J* = 4.1 Hz, 1H), 4.32 (t, *J* = 4.1 Hz, 1H), 4.69 (t, *J* = 4.1 Hz, 1H), 4.85 (t, *J* = 4.1 Hz, 1H), 6.36 (br s, 1H), 6.66 (d, *J* = 9.2 Hz, 2H); 6.83–7.00 (m, 4H), 7.676 (d, *J* = 9.2 Hz, 2H). Anal. (C₂₅H₃₅FN₄O₂·H₂C₂O₄) C, H, N.

4-(2-Fluoroethyl)-N-(4-(4-(2-(2-fluoroethoxy)phenyl)piperazin-1-yl)butyl)benzamide (20b)

20b was prepared from 4-(2-fluoroethyl)benzoic acid and **17b**. Yield: 95%. Mp (oxalate salt): 140.5–142.1 °C. ¹H NMR (free base, CDCl₃): δ 1.60–1.78 (m, 4H), 2.46 (t, *J* = 6.8 Hz, 2H), 2.63 (s, 4H), 3.00 (t, *J* = 6.4 Hz, 2H), 3.06–3.10 (m, 4H), 3.48 (q, *J* = 5.4 Hz, 2H), 4.20 (t, *J* = 4.2 Hz, 1H), 4.29 (t, *J* = 4.2 Hz, 1H), 4.54 (t, *J* = 6.4 Hz, 1H), 4.67–4.71 (m, 2H), 4.85 (t, *J* = 4.1 Hz, 1H), 6.72 (br s, 1H), 6.83–6.90 (m, 2H), 6.95–6.98 (m, 2H), 7.28 (d, *J* = 8.1 Hz, 2H), 7.71 (dd, *J* = 2.1, 6.3 Hz, 2H). Anal. (C₂₅H₃₃F₂N₃O₂·0.5H₂C₂O₄) C, H, N.

4-(2-Fluoroethoxy)-*N*-(4-(4-(2-(2-fluoroethoxy)phenyl)piperazin-1-yl)butyl)benzamide (20c)

20c was prepared from **9a** and **17b**. Yield: 80%. Mp (oxalate salt): 110.3–112.8 °C. ¹H NMR (free base, CDCl₃): δ 1.60–1.72 (m, 4H), 2.45 (t, *J* = 6.8 Hz, 2H), 2.63 (s, 4H), 3.10 (s, 4H), 3.47 (q, *J* = 5.7 Hz, 2H), 4.20 (t, *J* = 4.5 Hz, 2H), 4.28 (t, *J* = 4.5 Hz, 2H), 4.69 (t, *J* = 4.5 Hz, 2H), 4.83 (t, *J* = 4.5 Hz, 2H), 6.59 (br s, 1H), 6.83–7.00 (m, 6H), 7.73 (d, *J* = 9.0 Hz, 2H). Anal. (C₂₅H₃₃F₂N₃O₃·H₂C₂O₄) C, H, N.

4-(2-(2-Fluoroethoxy)ethoxy)-*N*-(4-(4-(2-(2-fluoroethoxy)phenyl)piperazin-1-yl)butyl)benzamide (20d)

20d was prepared from **12a** and **17b**. Yield: 77%. Mp (oxalate salt): 110.5–112.6 °C. ¹H NMR (free base, CDCl₃): δ 1.67–1.71 (m, 4H), 2.50 (t, *J* = 6.3 Hz, 2H), 2.68 (s, 4H), 3.13 (s, 4H), 3.47 (q, *J* = 5.4 Hz, 2H), 3.77 (t, *J* = 4.1 Hz, 1H), 3.85–3.91 (m, 3H), 4.16–4.21 (3.47) (m, 3H), 4.29 (t, *J* = 4.4 Hz, 1H), 4.51 (t, *J* = 4.1 Hz, 1H), 4.66–4.71 (4.69) (m, 2H), 4.85 (t, *J* = 4.1 Hz, 1H), 6.6159 (br s, 1H), 6.83–7.04 (m, 6H), 7.73 (d, *J* = 9.0 Hz, 2H). Anal. (C₂₇H₃₇F₂N₃O₄·H₂C₂O₄) C, H, N.

4-(Thiophen-3-yl)-*N*-(4-(4-(2-(2-fluoroethoxy)phenyl)piperazin-1-yl)butyl)benzamide (20e)

20e was prepared from 4-(thiophen-3-yl)benzoic acid and **17b**. Yield: 62%. Mp (oxalate salt): 193.3–194.1 °C. ¹H NMR (free base, CDCl₃): δ 1.68–1.72 (m, H), 2.48 (t, *J* = 6.0 Hz, 2H), 2.65 (s, 4H), 2.10 (s, 4H), 3.50 (q, *J* = 5.7 Hz, 2H), 4.19 (t, *J* = 4.2 Hz, 1H), 4.28 (t, *J* = 4.2 Hz, 1H), 4.69 (t, *J* = 4.2 Hz, 1H), 4.84 (t, *J* = 4.2 Hz, 1H), 6.79 (br s, 1H), 6.82–7.00 (m, 4H), 7.41 (d, *J* = 2.7 Hz, 2H), 7.52 (t, *J* = 2.7 Hz, 1H), 7.64 (d, *J* = 8.7 Hz, 2H), 7.80 (d, *J* = 8.7 Hz, 2H). Anal. (C₂₇H₃₂FN₃O₂S·H₂C₂O₄) C, H, N.

4-(2-(2-(2-Fluoroethoxy)ethoxy)ethoxy)-*N*-(4-(4-(2-(2-fluoroethoxy)phenyl)piperazin-1-yl)butyl) benzamide (20f)

20f was prepared from **12b** and **17b**. Yield: 82%. Mp (oxalate salt): 110.7–111.6 °C. ¹H NMR (free base, CDCl₃): δ 1.67–1.69 (m, 4H), 2.48 (t, *J* = 5.9 Hz, 3H), 2.67 (s, 4H), 3.12 (s, 4H), 3.47 (q, *J* = 5.4 Hz, 2H), 3.68–3.76 (m, 4H), 3.80 (t, *J* = 4.2 Hz, 1H), 3.87 (t, *J* = 4.8 Hz, 2H), 4.12 (t, *J* = 4.8 Hz, 2H), 4.20 (t, *J* = 4.2 Hz, 1H), 4.31 (t, *J* = 4.2 Hz, 1H), 4.48 (t, *J* = 4.2 Hz, 1H), 4.64 (t, *J* = 4.2 Hz, 1H), 4.69 (t, *J* = 4.2 Hz, 1H), 4.85 (t, *J* = 4.2 Hz, 1H), 6.55 (br s, 1H), 6.82–7.02 (m, 6H), 7.73 (d, *J* = 9.0 Hz, 2H). Anal. (C₂₉H₄₁F₂N₃O₅·H₂C₂O₄) C, H, N.

4-(Dimethylamino)-*N*-(4-(4-(2-(2-fluoroethoxy)phenyl)piperazin-1-yl)-*trans*-butyl-2-enyl)-benzamide (21a)

21a was prepared from 4-dimethylaminobenzoic acid and **17d**. Yield: 50%. Mp (oxalate salt): 84.9–85.9 °C. ¹H NMR (free base, CDCl₃) δ 2.66 (s, 4H), 3.01 (s, 6H), 3.07 (d, *J* = 4.5 Hz, 2H), 3.14 (s, 4H), 4.09 (t, *J* = 5.4 Hz, 2H), 4.21 (t, *J* = 4.2 Hz, 1H), 4.30 (t, *J* = 4.2 Hz, 1H), 4.70 (t, *J* = 4.2 Hz, 1H), 4.86 (t, *J* = 4.2 Hz, 1H), 5.76–5.80 (m, 2H), 6.05 (s, 1H), 6.66 (d, *J* = 9.0 Hz, 2H), 6.82–6.87 (m, 1H), 6.94–6.97 (m, 3H), 7.68 (d, *J* = 9.0 Hz, 2H). Anal. (C₂₅H₃₃FN₄O₂·H₂C₂O₄·H₂O) C, H, N.

4-(2-Fluoroethyl)-*N*-(4-(4-(2-(2-Fluoroethoxy)phenyl)piperazin-1-yl)-*trans*-butyl-2-enyl)benzamide (21b)

21b was prepared from 4-(2-fluoroethyl)benzoic acid and **17d**. Yield: 72%. Mp (oxalate salt): 155.0–156.1 °C. ¹H NMR (free base, CDCl₃): δ 2.67 (s, 4H), 3.01 (t, *J* = 4.1 Hz, 2H), 3.07–3.13 (m, 6H), 4.10 (t, *J* = 4.1 Hz, 2H), 4.20–4.20 (t, *J* = 4.1 Hz, 1H), 4.30 (t, *J* = 4.1 Hz, 1H), 4.57 (t, *J* = 6.3 Hz, 1H), 4.68–4.76 (m, 2H), 4.84 (t, *J* = 4.1 Hz, 1H), 5.76–5.80 (m, 2H), 6.18 (br s, 1H), 6.82–6.88 (m, 1H), 6.95–6.97 (m, 3H), 7.29 (d, *J* = 8.1 Hz, 2H), 7.704 (d, *J* = 8.1 Hz, 2H). Anal. (C₂₅H₃₁F₂N₃O₂·0.5H₂C₂O₄) C, H, N.

4-(2-Fluoroethoxy)-*N*-(4-(4-(2-(2-fluoroethoxy)-phenyl)-piperazin-1-yl)-*trans*-butyl-2-enyl)-benzamide (21c)

21c was prepared from **9a** and **17d**. Yield: 48%. Mp (oxalate salt): 112.8–125.1 °C. ¹H NMR (free base, CDCl₃): δ 2.68 (s, 4H), 3.09 (s, 3H), 3.15 (s, 3H), 4.10 (t, *J* = 4.2 Hz, 2H), 4.20 (t, *J* = 4.2 Hz, 2H), 4.30 (t, *J* = 4.2 Hz, 2H), 4.70 (t, *J* = 4.2 Hz, 2H), 4.86 (t, *J* = 4.2 Hz, 2H), 5.70–5.90 (m, 2H), 6.170 (br s, 1H), 6.81–6.85 (m, 1H), 6.93–7.00 (m, 5H), 7.75 (d, *J* = 10.5 Hz, 2H). Anal. (C₂₅H₃₁F₂N₃O₃·2H₂C₂O₄) C, H, N.

4-(2-(2-fluoroethoxy)ethoxy)-*N*-(4-(4-(2-(2-fluoroethoxy)phenyl)piperazin-1-yl)-*trans*-but-2-enyl)-benzamide (21d)

21d was prepared from **12a** and **17d**. Yield: 76%. Mp (oxalate salt): 113.4–115.0 °C. ¹H NMR (free base, CDCl₃): δ 2.67 (s, 4H), 3.08 (d, *J* = 2.7 Hz, 2H), 3.84–3.14 (s, 4H), 3.77 (t, *J* = 4.2 Hz, 1H), 3.86–3.96 (m, 3H), 4.08 (t, *J* = 4.2 Hz, 2H), 4.17–4.22 (m, 3H), 4.30 (t, *J* = 4.2 Hz, 1H), 4.52 (t, *J* = 4.2 Hz, 1H), 4.66–4.70 (m, 2H), 4.85 (t, *J* = 4.2 Hz, 1H), 5.77–5.80 (m, 2H), 6.11 (t, *J* = 8.7 Hz, 1H), 6.84–6.88 (m, 1H), 6.93–6.99 (m, 5H), 7.74 (td, *J* = 2.4, 9.0 Hz, 2H). Anal. (C₂₇H₃₅F₂N₃O₄·1.5H₂C₂O₄) C, H, N.

4-(Thiophen-3-yl)-*N*-(4-(4-(2-(2-fluoroethoxy)phenyl)piperazin-1-yl)-*trans*-but-2-enyl)benzamide (21e)

21e was prepared from 4-(thiophen-3-yl)benzoic acid and **17d**. Yield: 62%. Mp (oxalate salt): 140.5–142.1 °C. ¹H NMR (free base, CDCl₃): δ 2.66 (s, 4H), 3.08 (d, *J* = 4.0 Hz, 2H), 3.14 (s, 4H), 4.12 (t, *J* = 4.0 Hz, 2H), 4.22 (t, *J* = 4.0 Hz, 1H), 4.30 (t, *J* = 4.0 Hz, 1H), 4.70 (t, *J* = 4.0 Hz, 1H), 4.86 (t, *J* = 4.0 Hz, 1H), 5.80–5.82 (m, 2H), 6.23 (br s, 1H), 6.83–6.88 (m, 1H), 6.93–7.00 (m, 3H), 7.42 (d, *J* = 10.2 Hz, 2H), 7.54 (t, *J* = 2.1 Hz, 1H), 7.66 (td, *J* = 3.6, 10.5 Hz, 2H), 7.81 (td, *J* = 3.3, 13.2 Hz, 2H). The elemental analysis was conducted on free base of **21e**. Anal. (C₂₇H₃₀FN₃O₂S) C, H, N.

In Vitro Binding Studies

Dopamine receptor binding assays

The binding properties of membrane-associated receptors were characterized by a filtration binding assay.³⁴ For human D₂long, D₃, and D₄ dopamine receptors expressed in HEK 293 cells, 50 μL of membrane homogenates were suspended in 50 mM Tris–HCl/150 mM NaCl/10 mM EDTA buffer, pH = 7.5 and incubated with 50 μL of [¹²⁵I]IABN³⁴ at 37°C for 60 min, using 20 μM (+)-butaclamol to define the non-specific binding. The radioligand concentration was equal to approximately 0.5 times the *K_d* value and the concentration of the competitive inhibitor ranged over 5 orders of magnitude for competition experiments. For each competition curve, two concentrations of inhibitor per decade was used and triplicates were performed. Binding was terminated by the addition of the cold wash buffer (10mM Tris–HCl/150mM NaCl, pH = 7.5) and filtration over a glass-fiber filter (Schleicher and Schuell No. 32). A Packard Cobra gamma counter was used to measure the radioactivity. The equilibrium dissociation constant and maximum number of binding sites were generated using unweighted non-linear regression analysis of data modeled according to the equation describing mass action binding. The concentration of inhibitor that inhibits 50% of the specific binding of the radioligand (IC₅₀ value) was determined by using nonlinear regression analysis to analyze the data of competitive inhibition experiments. Competition curves were modeled for a single site and the IC₅₀ values were converted to equilibrium dissociation constants (*K_i* values) using the Cheng and Prusoff³⁵ correction. Mean *K_i* values ± S.E.M. are reported for at least three independent experiments.

Sigma Receptor Binding Assays

Before determining the σ_1 and σ_2 receptor binding assays, the compounds were dissolved in either DMF, DMSO, or ethanol and then diluted in 50 mM Tris-HCl buffer containing 150 mM NaCl and 100 mM EDTA at pH = 7.4. The procedures for isolating the membrane homogenates and performing the σ_1 and σ_2 receptor binding assays have been described previously.^{24, 33}

Briefly, the σ_1 receptor binding assays were conducted in 96-well plates using guinea pig brain membrane homogenates (~300 μg protein) and ~5 nM (+)-[³H]-pentazocine (34.9 Ci/mmol, Perkin Elmer, Boston, MA). The total incubation time was 90 min at room temperature. Nonspecific binding was determined from samples that contained 10 μM of cold haloperidol. After 90 min, the reaction was terminated by the adding 150 μL of ice-cold wash buffer (10 mM Tris-HCl, 150 mM NaCl, pH 7.4) using a 96 channel transfer pipette (Fisher Scientific, Pittsburgh, PA). The samples were harvested and filtered rapidly through a 96-well fiber glass filter plate (Millipore, Billerica, MA) that had been presoaked with 100 μL of 50 mM Tris-HCl buffer at pH = 8.0 for 1 h. Each filter was washed 3 times with 200 μL of ice-cold wash buffer, and the filter counted in a Wallac 1450 MicroBeta liquid scintillation counter (Perkin Elmer, Boston, MA).

The σ_2 receptor binding assays were conducted using rat liver membrane homogenates (~300 μg protein) and ~5 nM [³H]-DTG (58.1 Ci/mmol, Perkin Elmer, Boston, MA) in the presence of 1 μM (+)-pentazocine to block σ_1 sites. The incubation time was 2 h at room temperature. Nonspecific binding was determined from samples that contained 10 μM of cold haloperidol. All other procedures were identical to those described above for the σ_1 receptor binding assay.

Data from the competitive inhibition experiments were modeled using nonlinear regression analysis to determine the concentration that inhibits 50% of the specific binding of the radioligand (IC_{50} value). Competitive curves were best fit to a one-site fit and gave pseudo-Hill coefficients of 0.6–1.0. K_i values were calculated using Cheng and Prusoff method³⁵ and were presented as the mean \pm S.E.M. For these calculations, we used a K_d value of 7.89 nM for (+)-[³H]-pentazocine and guinea pig brain and a K_d value of 30.73 nM for [³H]-DTG and rat liver.²⁴

Whole cell adenylyl cyclase assay

The accumulation of ³H-cyclic AMP in HEK cells was measured by a modification of the Shimizu et al's method.³⁶ Transfected HEK cells were treated with serum-free media containing 2,8-[³H]adenine (ICN Pharmaceutical Inc., Costa Mesa, CA) and cells were incubated at 37°C for 75 min. Cells and drugs diluted in serum-free media containing 0.1 mM 3-isobutyl-1-methylxanthine (Sigma) were mixed to give a final volume of 500 μL and cells were incubated for 20 min at 37°C. The reaction was stopped by addition of 500 μL of 10% trichloroacetic acid and 1 mM cyclic AMP. After centrifugation, the supernatants were fractionated using Dowex AG1-X8 and neutral alumina to separate the [³H]ATP and the [³H]cyclic AMP. Individual samples were corrected for column recovery by monitoring the recovery of the cyclic AMP using spectrophotometric analysis at OD 259 nm.^{34, 36}

Supplementary Material

Refer to Web version on PubMed Central for supplementary material.

Acknowledgments

This work was supported by NIH grants DA16181 (RHM), DA23957 (RRL), and DA029840 (RHM).

References

1. Luedtke RR, Mach RH. Progress in developing D₃ dopamine receptor ligands as potential therapeutic agents for neurological and neuropsychiatric disorders. *Curr Pharm Des.* 2003; 9(8): 643–71. [PubMed: 12570797]
2. Sokoloff P, Giros B, Martres MP, Bouthenet ML, Schwartz JC. Molecular cloning and characterization of a novel dopamine receptor (D₃) as a target for neuroleptics. *Nature.* 1990; 347(6289):146–51. [PubMed: 1975644]
3. Reavill C, Taylor SG, Wood MD, Ashmeade T, Austin NE, Avenell KY, Boyfield I, Branch CL, Cilia J, Coldwell MC, Hadley MS, Hunter AJ, Jeffrey P, Jewitt F, Johnson CN, Jones DN, Medhurst AD, Middlemiss DN, Nash DJ, Riley GJ, Routledge C, Stemp G, Thewlis KM, Trail B, Vong AK, Hagan JJ. Pharmacological actions of a novel, high-affinity, and selective human dopamine D₃ receptor antagonist, SB-277011-A. *J Pharmacol Exp Ther.* 2000; 294(3):1154–65. [PubMed: 10945872]
4. Murray AM, Ryoo HL, Gurevich E, Joyce JN. Localization of dopamine D₃ receptors to mesolimbic and D₂ receptors to mesostriatal regions of human forebrain. *Proc Natl Acad Sci U S A.* 1994; 91(23):11271–5. [PubMed: 7972046]
5. Levesque D, Diaz J, Pilon C, Martres MP, Giros B, Souil E, Schott D, Morgat JL, Schwartz JC, Sokoloff P. Identification, characterization, and localization of the dopamine D₃ receptor in rat brain using 7-[³H]hydroxy-*N,N*-di-*n*-propyl-2-aminotetralin. *Proc Natl Acad Sci U S A.* 1992; 89(17):8155–9. [PubMed: 1518841]
6. Diaz J, Levesque D, Lammers CH, Griffon N, Martres MP, Schwartz JC, Sokoloff P. Phenotypical characterization of neurons expressing the dopamine D₃ receptor in the rat brain. *Neuroscience.* 1995; 65(3):731–45. [PubMed: 7609872]
7. Hall H, Halldin C, Dijkstra D, Wikstrom H, Wise LD, Pugsley TA, Sokoloff P, Pauli S, Farde L, Sedvall G. Autoradiographic localisation of D₃-dopamine receptors in the human brain using the selective D₃-dopamine receptor agonist (+)-[³H]PD 128907. *Psychopharmacology (Berl).* 1996; 128(3):240–7. [PubMed: 8972543]
8. Bordet R, Ridray S, Schwartz JC, Sokoloff P. Involvement of the direct striatonigral pathway in levodopa-induced sensitization in 6-hydroxydopamine-lesioned rats. *Eur J Neurosci.* 2000; 12(6): 2117–23. [PubMed: 10886351]
9. Bordet R, Ridray S, Carboni S, Diaz J, Sokoloff P, Schwartz JC. Induction of dopamine D₃ receptor expression as a mechanism of behavioral sensitization to levodopa. *Proc Natl Acad Sci U S A.* 1997; 94(7):3363–7. [PubMed: 9096399]
10. Bordet R. Central dopamine receptors: general considerations (Part 1). *Rev Neurol (Paris).* 2004; 160:8–9. 862–70.
11. Kumar R, Riddle L, Griffin SA, Grundt P, Newman AH, Luedtke RR. Evaluation of the D₃ dopamine receptor selective antagonist PG01037 on l-dopa-dependent abnormal involuntary movements in rats. *Neuropharmacology.* 2009; 56:6–7. 944–955. [PubMed: 18765242]
12. Cenci MA. Dopamine dysregulation of movement control in L-DOPA-induced dyskinesia. *Trends Neurosci.* 2007; 30(5):236–43. [PubMed: 17400300]
13. Mela F, Millan MJ, Brocco M, Morari M. The selective D₃ receptor antagonist, S33084, improves parkinsonian-like motor dysfunction but does not affect l-DOPA-induced dyskinesia in 6-hydroxydopamine hemi-lesioned rats. *Neuropharmacology.* 2010; 58(2):528–536. [PubMed: 19733554]
14. Visanji NP, Fox SH, Johnston T, Reyes G, Millan MJ, Brotchie JM. Dopamine D₃ receptor stimulation underlies the development of L-DOPA-induced dyskinesia in animal models of Parkinson's disease. *Neurobiology of Disease.* 2009; 35(2):184–192. [PubMed: 19118628]
15. Vingerhoets FJG. Dyskinesia in Parkinson disease: Back for the future. *Neurology.* 2009; 72(14): 1202–1203. [PubMed: 19349599]
16. Sokoloff P, Le Foll B, Perachon S, Bordet R, Ridray S, Schwartz JC. The dopamine D₃ receptor and drug addiction. *Neurotox Res.* 2001; 3(5):433–41. [PubMed: 14715457]

17. Van Kampen JM, Eckman CB. Dopamine D₃ receptor agonist delivery to a model of Parkinson's disease restores the nigrostriatal pathway and improves locomotor behavior. *J Neurosci*. 2006; 26(27):7272–80. [PubMed: 16822985]
18. Pilla M, Perachon S, Sautel F, Garrido F, Mann A, Wermuth CG, Schwartz JC, Everitt BJ, Sokoloff P. Selective inhibition of cocaine-seeking behaviour by a partial dopamine D₃ receptor agonist. *Nature*. 1999; 400(6742):371–5. [PubMed: 10432116]
19. Khaled MATM, Farid Araki K, Li B, Coen KM, Marinelli PW, Varga J, Gaál J, Le Foll B. The selective dopamine D₃ receptor antagonist SB 277011-A, but not the partial agonist BP 897, blocks cue-induced reinstatement of nicotine-seeking. *Int J Neuropsychopharmacol*. 2009:1–10.
20. Grundt P, Carlson EE, Cao J, Bennett CJ, McElveen E, Taylor M, Luedtke RR, Newman AH. Novel heterocyclic trans olefin analogues of *N*-{4-[4-(2,3-dichlorophenyl)piperazin-1-yl]butyl}arylcarboxamides as selective probes with high affinity for the dopamine D₃ receptor. *J Med Chem*. 2005; 48(3):839–48. [PubMed: 15689168]
21. Garcia-Ladona FJ, Cox BF. BP 897, a selective dopamine D₃ receptor ligand with therapeutic potential for the treatment of cocaine-addiction. *CNS Drug Reviews*. 2003; 9(2):141–158. [PubMed: 12847556]
22. Carr KD, Yamamoto N, Omura M, Cabeza de Vaca S, Krahn L. Effects of the D₃ dopamine receptor antagonist, U99194A, on brain stimulation and d-amphetamine reward, motor activity, and c-fos expression in ad libitum fed and food-restricted rats. *Psychopharmacology (Berl)*. 2002; 163(1):76–84. [PubMed: 12185403]
23. Ghosh B, Antonio T, Zhen J, Kharkar P, Reith MEA, Dutta AK. Development of (*S*)-*N*⁶-(2-(4-(isoquinolin-1-yl)piperazin-1-yl)ethyl)-*N*⁶-propyl-4,5,6,7-tetrahydrobenzo[d]-thiazole-2,6-diamine and its analogue as a D₃ receptor preferring agonist: Potent in vivo activity in Parkinson's disease animal models. *J Med Chem*. 2010; 53(3):1023–1037. [PubMed: 20038106]
24. Chu W, Tu Z, McElveen E, Xu J, Taylor M, Luedtke RR, Mach RH. Synthesis and in vitro binding of *N*-phenyl piperazine analogs as potential dopamine D₃ receptor ligands. *Bioorg Med Chem*. 2005; 13(1):77–87. [PubMed: 15582454]
25. Chen J, Collins GT, Zhang J, Yang CY, Levant B, Woods J, Wang S. Design, synthesis, and evaluation of potent and selective ligands for the dopamine 3 (D₃) receptor with a novel in vivo behavioral profile. *J Med Chem*. 2008; 51(19):5905–8. [PubMed: 18785726]
26. Bettinetti L, Schlotter K, Hubner H, Gmeiner P. Interactive SAR studies: rational discovery of super-potent and highly selective dopamine D₃ receptor antagonists and partial agonists. *J Med Chem*. 2002; 45(21):4594–7. [PubMed: 12361386]
27. Hackling A, Ghosh R, Perachon S, Mann A, Holtje HD, Wermuth CG, Schwartz JC, Sippl W, Sokoloff P, Stark H. *N*-(ω-(4-(2-methoxyphenyl)piperazin-1-yl)alkyl)carboxamides as dopamine D₂ and D₃ receptor ligands. *J Med Chem*. 2003; 46(18):3883–99. [PubMed: 12930150]
28. Hocke C, Prante O, Salama I, Hubner H, Lober S, Kuwert T, Gmeiner P. ¹⁸F-Labeled FAUC 346 and BP 897 derivatives as subtype-selective potential PET radioligands for the dopamine D₃ receptor. *ChemMedChem*. 2008; 3(5):788–93. [PubMed: 18306190]
29. Leopoldo M, Lacivita E, De Giorgio P, Colabufo NA, Niso M, Berardi F, Perrone R. Design, synthesis, and binding affinities of potential positron emission tomography (PET) ligands for visualization of brain dopamine D₃ receptors. *J Med Chem*. 2006; 49(1):358–65. [PubMed: 16392820]
30. Gao M, Wang M, Hutchins GD, Zheng QH. Synthesis of new carbon-11-labeled carboxamide derivatives as potential PET dopamine D₃ receptor radioligands. *Appl Radiat Isot*. 2008; 66(12):1891–7. [PubMed: 18602269]
31. Xu J, Chu W, Tu Z, Jones LA, Luedtke RR, Perlmutter JS, Mintun MA, Mach RH. [³H]4-(Dimethylamino)-*N*-[4-(4-(2-methoxyphenyl)piperazin-1-yl)butyl]benzamide, a selective radioligand for dopamine D₃ receptors. I. In vitro characterization. *Synapse*. 2009; 63(9):717–28. [PubMed: 19425052]
32. Taylor M, Grundt P, Griffin SA, Newman AH, Luedtke RR. Dopamine D₃ receptor selective ligands with varying intrinsic efficacies at adenylyl cyclase inhibition and mitogenic signaling pathways. *Synapse*. 2010; 64(3):251–66. [PubMed: 19924694]

33. Grundt P, Prevatt KM, Cao J, Taylor M, Floresca CZ, Choi JK, Jenkins BG, Luedtke RR, Newman AH. Heterocyclic analogues of *N*-(4-(4-(2,3-dichlorophenyl)piperazin-1-yl)butyl) arylcarboxamides with functionalized linking chains as novel dopamine D₃ receptor ligands: Potential substance abuse therapeutic agents. *J Med Chem.* 2007; 50(17):4135–4146. [PubMed: 17672446]
34. Luedtke RR, Freeman RA, Boundy VA, Martin MW, Huang Y, Mach RH. Characterization of ¹²⁵I-IABN, a novel azabicyclononane benzamide selective for D₂-like dopamine receptors. *Synapse.* 2000; 38(4):438–49. [PubMed: 11044891]
35. Cheng Y, Prusoff WH. Relationship between the inhibition constant (K_i) and the concentration of inhibitor which causes 50 per cent inhibition (I_{50}) of an enzymatic reaction. *Biochem Pharmacol.* 1973; 22(23):3099–108. [PubMed: 4202581]
36. Shimizu H, Daly JW, Creveling CR. A radioisotopic method for measuring the formation of adenosine 3',5'-cyclic monophosphate in incubated slices of brain. *J Neurochem.* 1969; 16(12): 1609–19. [PubMed: 4314281]

Abbreviations

CIMS	Chemical ionization mass spectrometry
DCC	<i>N,N'</i> -Dicyclohexylcarbodiimide
DMF	<i>N,N</i> -Dimethylformamide
DMSO	Dimethyl sulfoxide
DAST	diethylaminosulfur trifluoride
DTG	1,3-Di-tolylguanidine
GIRKs	G protein-coupled inwardly-rectifying potassium channels
HEK cells	Human Embryonic Kidney 293 cells
[¹²⁵I]IABN	[¹²⁵ I] <i>N</i> -benzyl-5-iodo-2,3,-dimethoxy-[3.3.1]azabicyclononan-3-β-yl-benzamide
LID	L-DOPA-induced dyskinesia
PET	Positron Emission Tomography
PLD	Phospholipase D
SPECT	Single photon emission computed tomography
TBAF	Tetra- <i>n</i> -butylammonium fluoride

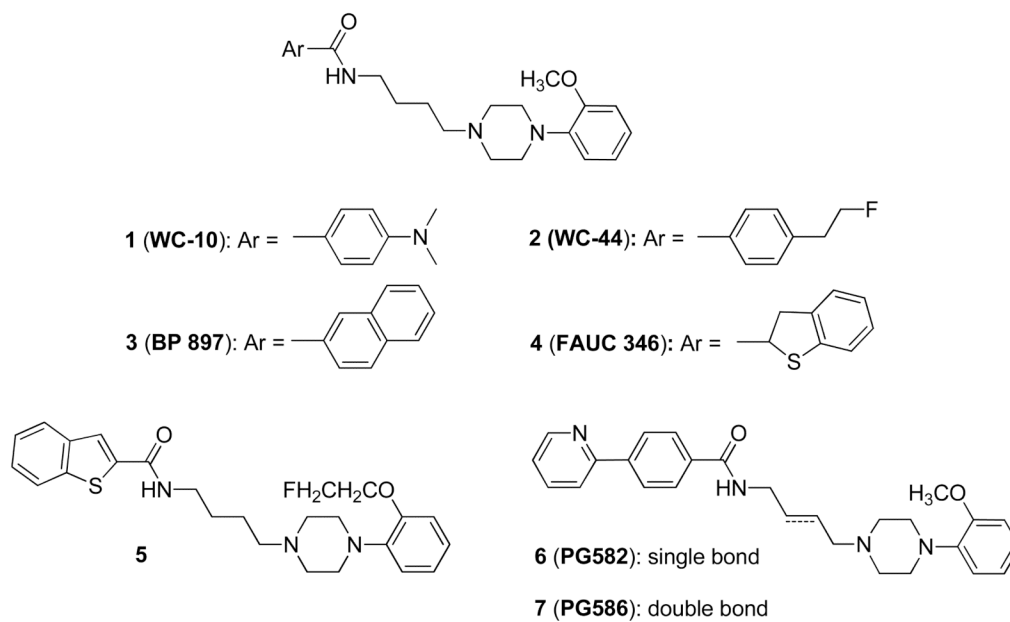
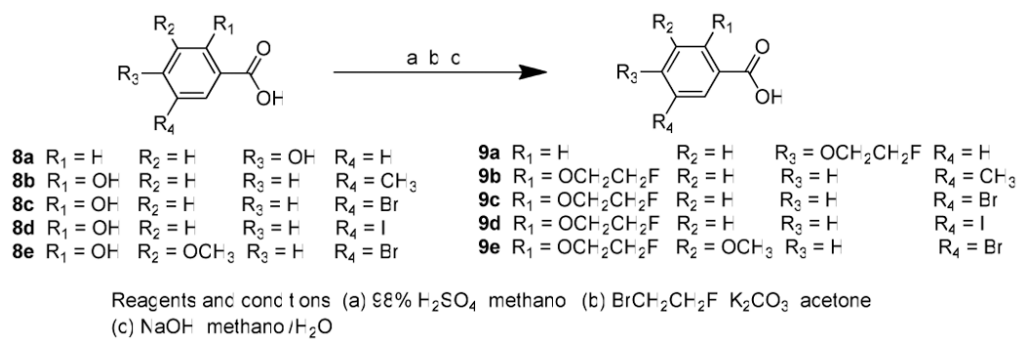
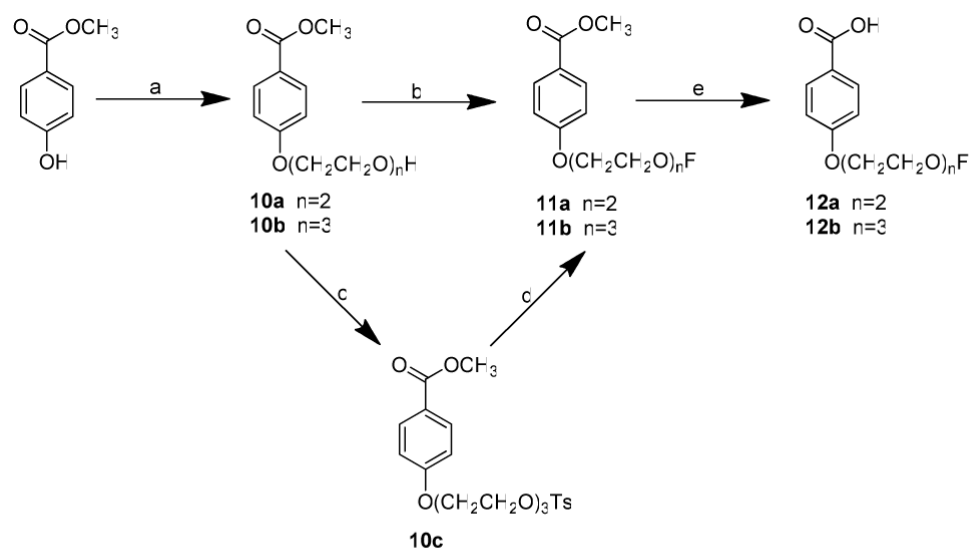


Figure 1.
Representative dopamine D₃ receptor ligands.

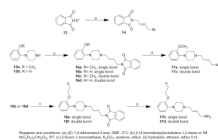


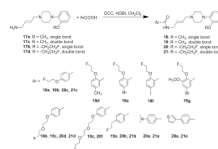
Scheme 1.



Reagents and conditions (a) 2-(2-chloroethoxy)ethanol or 2-(2-(2-chloroethoxy)ethoxy)ethanol, K_2CO_3 , THF
 (b) DAST, CH_2Cl_2 , 0°C (c) Triethylamine, p-toluenesulfonyl chloride, CH_2Cl_2 (d) TBAF/THF, reflux 4hr
 (e) NaOH, methanol/ H_2O

Scheme 2.

**Scheme 3.**



Scheme 4.

Table 1

D₂, D₃ and D₄ Affinities ($K_i \pm$ SD, nM) of the benzamide analogs.

	D ₂	D ₃	D ₄	D ₂ /D ₃ Ratio	Log p ^a
1	34.4 ± 4.7	0.8 ± 0.1	896 ± 272	43	3.09
2	54.5 ± 4.4	2.4 ± 0.4	804 ± 46	23	2.94
18a	27.1 ± 3.5	1.1 ± 0.1	1,400 ± 320	25	3.48
18b	20.9 ± 3.7	6.2 ± 0.9	ND	3.4	3.08
18c	52.0 ± 6.6	4.2 ± 0.2	2,100 ± 380	12.2	2.72
19a	131 ± 13	24.9 ± 3.3	ND	5.2	3.43
19b	55.3 ± 6.0	6.2 ± 0.3	ND	8.9	3.55
19c	59.2 ± 5.8	18.2 ± 2.3	ND	3.3	3.16
19d	17.8 ± 0.8	18.5 ± 2.4	ND	1	3.66
19e	13.4 ± 2.3	13.6 ± 2.0	ND	1	4.49
19f	13.2 ± 0.8	10.9 ± 1.5	ND	1.2	4.73
19g	57.6 ± 3.7	13.8 ± 1.2	ND	4.2	4.15
20a	15.1 ± 1.7	0.65 ± 0.2	890 ± 100	23	3.75
20b	21.4 ± 2.9	6.9 ± 1.0	ND	3.1	3.68
20c	15.1 ± 2.7	0.52 ± 0.03	990 ± 200	29	3.73
20d	14.2 ± 1.9	2.5 ± 0.3	ND	5.7	3.34
20e	27.7 ± 5.4	0.17 ± 0.01	246 ± 13	163	4.67
20f	31.7 ± 2.1	5.2 ± 0.3	ND	6.1	2.98
21a	35.2 ± 2.5	3.6 ± 0.6	ND	9.8	3.83
21b	17.7 ± 2.7	1.1 ± 0.2	890 ± 380	16.1	3.61
21c	37.9 ± 5.0	8.4 ± 1.3	ND	4.5	3.81
21d	64.8 ± 8.4	19.6 ± 3.2	ND	3.3	3.41
21e	70.5 ± 9.6	1.1 ± 0.2	182 ± 5	64	4.74
21f	25.9 ± 2.4	11.2 ± 2.2	ND	2.3	3.26
21g	10.9 ± 0.4	6.7 ± 1.1	ND	1.6	3.72
21h	12.0 ± 0.6	3.1 ± 0.3	ND	3.9	4.36

^aCalculated using ACD log D software, Advanced Chemistry Development, Toronto, Canada.

Table 2

Sigma Receptor Affinities ($K_i \pm SD$ [nM]) of Selected Analogs

	D_3	σ_1	σ_2	D_3/σ_1 Ratio	D_3/σ_2 Ratio	D_3/σ_2 ratio
1	0.8 \pm 0.1	1,260 \pm 290	1,570 \pm 310	1,573	1,970	1,970
2	2.4 \pm 0.4	3,540 \pm 2500	2,210 \pm 260	1,476	919	919
18a	1.1 \pm 0.1	4,780 \pm 730	660 \pm 36	4344	601	601
18c	4.2 \pm 0.2	4,870 \pm 470	1,120 \pm 30	1,159	266	266
20a	0.65 \pm 0.2	1,960 \pm 50	650 \pm 38	3,017	1,002	1,002
20c	0.52 \pm 0.03	4,360 \pm 570	794 \pm 14	8,377	1,527	1,527
20e	0.17 \pm 0.01	20,900 \pm 5250	5,960 \pm 360	122,706	35,047	35,047
21b	1.1 \pm 0.2	7,200 \pm 880	2,020 \pm 260	6,541	1,839	1,839
21e	1.1 \pm 0.2	7,780 \pm 540	1,320 \pm 33	7,076	1,200	1,200
Haloperidol	–	1.5 \pm 0.3	24.2 \pm 3.0	–	–	–

Table 3
Intrinsic Efficacy of Selected Analogues at Dopamine D₂ and D₃ Receptors^a

Compound	hD ₂ HEK	hD ₃ HEK
Haloperidol	-0.6 ± 1.6	4.0 ± 5.5
1	33.5 ± 3.1	18.7 ± 2.2
2	35.3 ± 1.0	96.2 ± 4.2
18a	58.6 ± 1.1	68.8 ± 5.6
18c	63.8 ± 4.2	59.9 ± 7.4
20a	66.3 ± 1.0	64.5 ± 8.3
20c	73.2 ± 0.7	50.3 ± 5.2
20e	29.3 ± 7.3	34.5 ± 1.7
21b	65.8 ± 0.2	65.5 ± 7.2
21e	21.2 ± 5.5	55.4 ± 4.2
Quinpirole	100	100

^aThe intrinsic efficacy of the test compounds was evaluated by determining the percent inhibition of a forskolin-dependent whole cell adenylyl cyclase assay. The results were normalized to the percent inhibition obtained using the full agonist quinpirole at human D₂ (1 μM) and D₃ (100 nM) receptors expressed in stably transfected HEK 293 cells. For D₂ receptors the maximum inhibition was >90% and for D₃ receptors the maximum inhibition ranged from 38 to 53%. The test drug was used at a concentration equal to approximately 10 × the K_i value that was determined from the radioligand binding analysis. The mean ± the S.E.M. values are reported for n ≥ 3.